2014

Molecular Opacities for Exoplanets

P. F. Bernath
Old Dominion University

Original Publication Citation

Bernath, P. F. (2014). Molecular opacities for exoplanets. *Philosophical Transactions of the Royal Society A: Mathematical, Physical, and Engineering Sciences, 372*(2014), 20130087 doi:10.1098/rsta.2013.0087

PHILOSOPHICAL TRANSACTIONS OF THE ROYAL SOCIETY A

rsta.royalsocietypublishing.org

Discussion

Cite this article: Bernath PF. 2014 Molecular opacities for exoplanets. *Phil. Trans. R. Soc. A* **372**: 20130087.
http://dx.doi.org/10.1098/rsta.2013.0087

One contribution of 17 to a Theo Murphy Meeting Issue 'Characterizing exoplanets: detection, formation, interiors, atmospheres and habitability'.

Subject Areas:
extrasolar planets

Keywords:
exoplanet spectroscopy, hot Jupiters, super-Earths, infrared spectroscopy, laboratory astrophysics, molecular opacities

Author for correspondence:
Peter F. Bernath
e-mail: peter.bernath@york.ac.uk

Royal Society Publishing

Molecular opacities for exoplanets

Peter F. Bernath[1,2]

[1]Department of Chemistry and Biochemistry, Old Dominion University, Norfolk, VA 23508, USA
[2]Department of Chemistry, University of York, Heslington, York YO10 5DD, UK

Spectroscopic observations of exoplanets are now possible by transit methods and direct emission. Spectroscopic requirements for exoplanets are reviewed based on existing measurements and model predictions for hot Jupiters and super-Earths. Molecular opacities needed to simulate astronomical observations can be obtained from laboratory measurements, *ab initio* calculations or a combination of the two approaches. This discussion article focuses mainly on laboratory measurements of hot molecules as needed for exoplanet spectroscopy.

1. Introduction

The first exoplanet, a 'hot Jupiter' orbiting around the star 51 Pegasi, was discovered by Mayor & Queloz in 1995 by the radial velocity method [1]. The parent star is classified as G2V and is very similar to the Sun, but the 51 Pegasi b planet is very strange by the standards of our own Solar System. 51 Peg b has a mass of about 0.5 M_J (mass of Jupiter), but is located at 0.05 AU and has an orbital period of 4.2 days. It is as if Jupiter were to be transported in our Solar System so that it was seven times closer to the Sun than Mercury. The composition of 51 Peg b is expected to be similar to that of Jupiter but with a surface temperature of about 1300 K rather than about 125 K for Jupiter.

Almost all of the hundreds of exoplanets (see http://exoplanet.eu/) have been detected or confirmed by observing periodic Doppler shifts in the spectrum of the parent star [1,2]. A star and a planet orbit about a common centre of mass and this motion causes the parent star to periodically move away and towards the observer. It is not possible to determine the inclination angle of the orbital plane from the Doppler effect, but these observations give the orbital radius, eccentricity of

the orbit and a lower limit for the mass of the planet (as long as the stellar mass is known). The Doppler shifts are the largest for large planets close to the parent star, so there is a selection effect that favours the detection of hot Jupiters.

If the orbital inclination of an exoplanet is close to 90°, then the planet can transit the star and be detected by the small decrease in light as the planet passes in front of the star. The hot Jupiter HD 209458b was the first transiting planet observed with a dip in light intensity of about 1.5% [3]. This type of precision photometry is best done from orbit, for example using the Hubble Space Telescope, and the Kepler mission (http://kepler.nasa.gov/) which searched for Earth-like planets by their transits. Kepler has detected thousands of exoplanet candidates [4] that need to be confirmed by other methods, for example the radial velocity technique. The combination of Doppler and transit data allows for a rather complete description of a planet including orbit inclination, planetary mass, radius and density.

While the detection of more than 1000 exoplanets by the end of 2013 is a remarkable achievement, it is the spectroscopy of these objects that has excited the most interest. The technique of 'transit spectroscopy' allows the detection of molecular absorptions in exoplanets. The idea is simple: the effective size of a planet with an atmosphere depends on the wavelength because the planet appears bigger at a strongly absorbing wavelength than at a wavelength for which the atmosphere is transparent. By measuring very precisely the size of the dips in the stellar radiation during transit as a function of wavelength, a spectrum of the planet is obtained. The technique is also called transmission spectroscopy because the variation in the size of the dips is associated with light that is transmitted through the atmosphere. For example, Swain *et al*. [5] observed the transiting exoplanet HD 189733b with the Hubble Space Telescope using the NICMOS camera in the 1.4–2.5 μm range. HD 189733b is a hot-Jupiter planet in a 2.2 day orbit around a bright K2V primary star. A model atmosphere of mainly molecular hydrogen with a water relative abundance of 5×10^{-4} and a methane abundance of 5×10^{-5} was needed to match the observed wavelength dependence of the transit dips. They used the BT2 line list [6] for water and a combination of HITRAN [7] and Nassar & Bernath [8] for methane.

Direct spectroscopic measurement of the radiation emitted by exoplanets has also been demonstrated. For example, the 'emergent flux' from HD 189733b was directly detected [9] with a similar instrument configuration as used for transit spectroscopy [5]. The NICMOS instrument on Hubble was used again for imaging spectroscopy with a resolving power of 40 in the 1.4–2.5 μm range. In essence, Swain *et al*. [9] manipulate the spectra recorded just before the planet disappears behind the star (i.e. star plus planet) and spectra recorded during occultation with the planet behind the star (i.e. star only) to obtain the emission spectrum of the planet alone. The planetary flux contained modulations that required the addition of H_2O, CO and CO_2 to their model atmosphere. The interpretation of such spectra is not straightforward because the molecular bands could appear in absorption or emission or both, depending on the details of the atmospheric pressure–temperature height profile and the composition of the different atmospheric layers. The non-detection of methane is explained as being because of the different atmospheric regions sampled by emission spectroscopy (dayside emission from higher pressure and temperature regions) as compared with transit spectroscopy (sampling of lower pressure cooler outer regions in the terminator between night and day).

The Infrared Spectrograph on the Spitzer Space Telescope was used by Grillmair *et al*. [10] to record emission spectra of HD 189733b in the thermal infrared that supports the detection of water vapour. Ground-based observations are also possible for this object and the work of Waldmann *et al*. [11] suggests methane emission at 3.3 μm. Although HD 189733b is the most studied object, spectra have been recorded for a number of other hot Jupiters, for example HD 209458b [12].

In addition to hot Jupiters, planets with masses in the range of about 2–10 Earth masses (i.e. between the size of the Earth and Neptune) have been discovered and have been dubbed 'super-Earths' [13]. Many of them have very short orbital periods like hot Jupiters and are also hot because of proximity to their parent star. For example, GJ 1214b has a mass 6.55 times that of the Earth, a density of 1.88 g cm^{-3} and an estimated equilibrium surface temperature of 555 K; Kepler-10b has a mass 4.54 times that of the Earth, a density of 8.74 g cm^{-3} and a surface temperature

of 1833 K [14]. The observation of super-Earths was a surprise (at least to planet formation modellers) because rocky planets close to the parent star were predicted to be smaller than the Earth [13].

Spectroscopy of exoplanets is extraordinarily difficult because of the overwhelming radiation from the parent star. The measurements require an unprecedented degree of photometric stability and correction of systematic errors at the level of 10^{-4} of the signal. Not unexpectedly, some of the work has been greeted with scepticism, but on the whole the detections have been confirmed. Exoplanets have captured the imagination of scientists and the general public, in part because they are first steps in the search for life on other worlds.

2. Spectroscopic requirements

The interpretation of spectroscopic measurements of exoplanets is much like the analysis of remote sensing data for the Earth's atmosphere. A model atmosphere is constructed with a certain composition and physical parameters, for example an altitude profile of temperature as a function of pressure. The model atmosphere is used to predict the observed spectrum ('forward model') and parameters, for example volume mixing ratios of atmospheric constituents, are adjusted until the model and observations agree. This retrieval problem, however, is very under-constrained (i.e. the information content of the spectrum is not high enough to determine all of the required parameters in the model) so various assumptions need to be made in order to obtain a solution [15]. Exoplanet models of observed spectra are plagued by 'degeneracy' in that very different models can give nearly the same spectra. A crucial part of the model atmosphere is the spectroscopic data used for the opacities in the radiative transfer calculation. Clearly, unreliable spectroscopic data will lead to the retrieval of incorrect compositions and physical properties for exoplanets.

What basic molecular spectroscopic data are required to interpret exoplanet spectra? The atmospheric temperatures and pressures can be estimated from general circulation models (GCMs, three-dimensional climate models) of heavily irradiated Jupiter-like planets [16]. The temperature range (figure 1) for a hot Jupiter like HD 189733b is about 500–1700 K and for the hotter HD 209458b, the maximum temperature is about 2800 K [17]. GCMs typically assume thermodynamic equilibrium [16] in order to obtain the atmospheric composition, but non-equilibrium chemistry is likely for these heavily irradiated objects. More sophisticated models include photochemistry [17] and predict atmospheric composition profiles for HD 189733b as displayed in figure 2. Molecular opacities are needed for H_2, CO, H_2O, N_2, CH_4, NH_3, CO_2 and HCN, in decreasing order of abundance.

More than 30 super-Earths have been discovered and the most interesting objects are rocky planets such as CoRoT-7b [18], which has an equilibrium temperature of 1810 K [14]. Schaefer *et al*. [14] have calculated the chemical equilibrium composition of super-Earths with temperatures in the range of 500–4000 K based on the vaporization of silicate rocks similar to those of the Earth's continental crust and bulk silicate Earth. The composition of the atmosphere at a pressure of 100 bar is presented as figure 3 for bulk silicate Earth. In addition to H_2O, CO_2, CH_4, CO and H_2 found in hot Jupiters, additional species such as SO_2, O_2, HCl, HF, NaCl, KCl, KF, KOH and NaOH are expected to appear.

What is required for the molecular species listed above are line lists suitable for temperatures up to about 2500 K. To include a molecular line in a radiative transfer calculation (at a certain temperature) requires three quantities: line position, line strength and line shape [19]. For a line shape, it is usually satisfactory to use a Voigt function, which is the convolution of a Gaussian for Doppler broadening and a Lorentzian for pressure broadening, given a temperature and a reasonable estimate for the collisional broadening parameter. The line intensity S' (in SI units of $m^2\,s^{-1}$ molecule^{-1}) at temperature T is given by the expression

$$S' = \frac{2\pi^2 \nu_{10} S_{J'J''}}{3\varepsilon_0 hcQ} \exp\left(-\frac{E_{\mathrm{Low}}}{kT}\right)\left[1 - \exp\left(-\frac{h\nu_{10}}{kT}\right)\right],$$

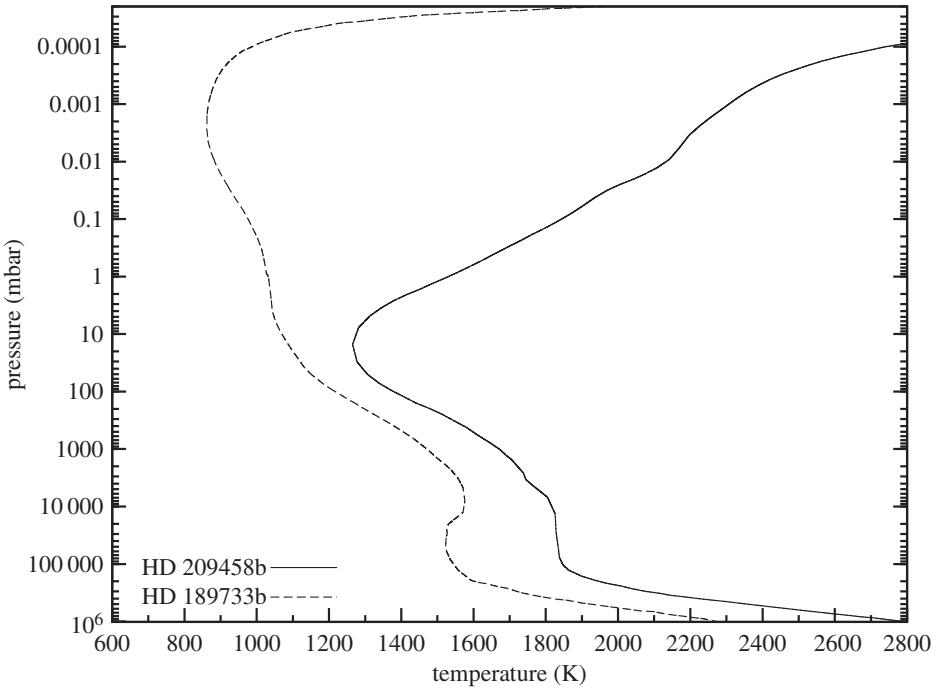

Figure 1. Estimated temperature profiles for the hot Jupiters HD 209458b and HD 189733b [17].

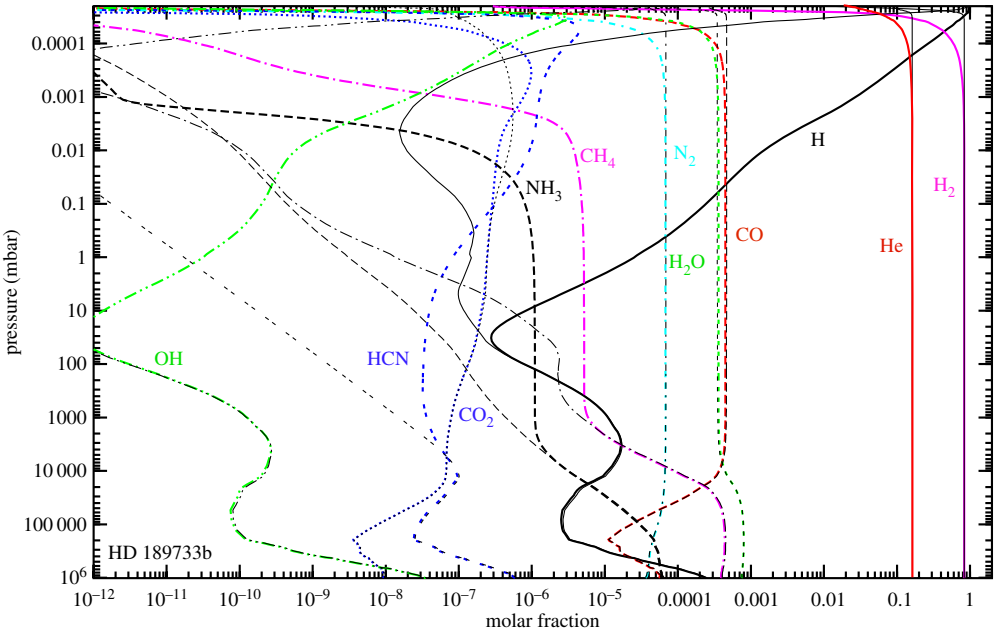

Figure 2. Composition of HD 189733b as a function of altitude (pressure) as calculated by Venot *et al*. [17]. (Online version in colour.)

in which $S_{J'J''}$ is the intrinsic line strength (square of the transition dipole moment), Q is the internal partition function and E_{Low} is the lower state energy of the transition at frequency ν_{12} [19]. As the partition function can be calculated from statistical thermodynamics [20], only three quantities are needed for a line: the line intensity S' (or $S_{J'J''}$), the lower state energy E_{Low} and the transition frequency ν_{10}.

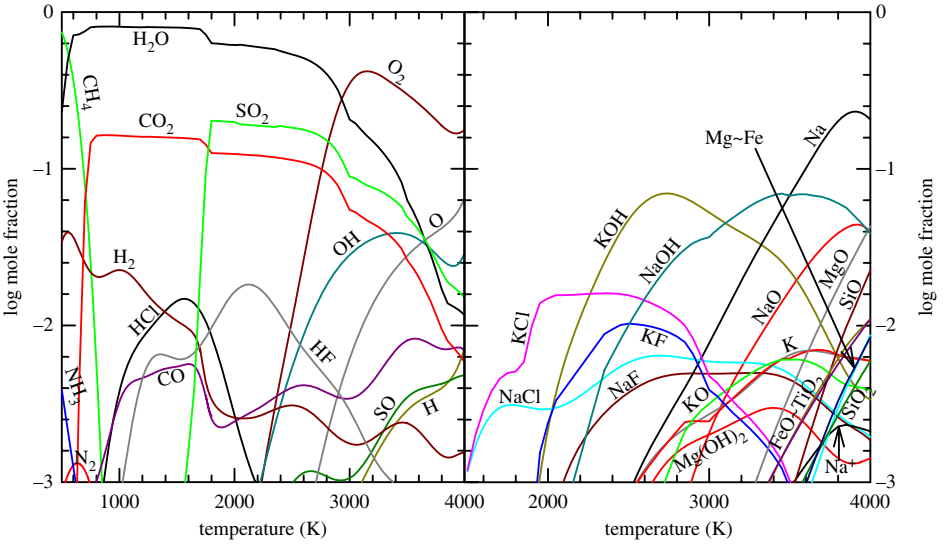

Figure 3. Gas composition at 100 bar as a function of temperature for bulk silicate Earth [14]. (Online version in colour.)

3. Molecular opacities

The high temperatures of most exoplanets present a major problem because millions of lines are needed to obtain reliable opacities. It is not feasible to obtain millions of line parameters from laboratory observations alone: they must be provided by theory. Yet, the purely theoretical calculation of molecular opacities is also not satisfactory because, except for molecular hydrogen, *ab initio* quantum chemistry is not yet sufficiently accurate. In other words, laboratory measurements alone do not provide sufficient lines while purely theoretical calculations do provide enough lines, but not with enough accuracy. The best opacities are therefore given by combining experiment and theory, for example, by the substitution of experimental line parameters in a more extensive calculated list. In essence, the strongest lines seen at high resolution come from laboratory data, but the millions of weaker lines that provide a kind of 'continuum' absorption come largely from theory. Molecular opacities have been reviewed by Sharp & Burrows [21] and Tennyson has begun a major project called ExoMol to compute them [22].

Line lists suitable for computing molecular opacities for exoplanets are available for many of the main species. For example, spectra of CO and CO_2 at high temperature are generally satisfactory and can be obtained for example from the HITEMP database [23], which is a high-temperature analogue of HITRAN. The HITRAN database [7] is aimed at simulating spectra of the Earth's atmosphere and is reliable at temperatures of 300 K or less. In the absence of more suitable data, HITRAN is often used although it is missing many hot bands, and the pressure broadening parameters are for air rather than molecular hydrogen.

Experimental spectral data for hot gases have an important role to play in exoplanet spectroscopy. In the absence of complete and reliable theoretical calculations, the laboratory data can be used directly to obtain molecular opacities. The laboratory observations serve to test and validate the more extensive calculated line lists. Finally, the experimental measurements can lead to improvements in the calculated line lists by empirical adjustment of the potential energy and dipole surfaces used to calculate the line lists, or by adding them to the calculated line lists or just by spurring the modellers to improve their calculations.

The example of water vapour line is illustrative of experimental work on hot gases. At 5800 K, the solar photosphere is too hot for H_2O to exist; the high-resolution ACE solar spectrum [24] (http://www.ace.uwaterloo.ca/) displays CO, OH, NH and CH absorption lines. Sunspots are cooler and their infrared spectra show a dense forest of absorption lines. By comparing a

laboratory emission spectrum of hot water vapour with the sunspot spectrum, it was possible to assign the carrier of the lines as hot water vapour ('Water on the Sun' [25]). The assignment of quantum numbers of the lines (needed to obtain lower state energies) was not possible using previous experimental or theoretical work. Tennyson and co-workers [26] were then able to assign most of the lines by computing the energy levels and line intensities by variational solution of the vibration–rotation Schrödinger equation with an *ab initio* potential energy function. This success led to more experimental observations in other spectral regions and at higher temperatures (3000 K in an oxyacetylene torch) and to increasingly accurate theoretical predictions. The experimental [27] and theoretical work [28] continues, but Barber *et al*. [6] have computed about half a billion water lines using an *ab initio* potential energy surface adjusted slightly to reproduce experimental observations and an *ab initio* dipole surface. The Barber *et al*. BT2 line list is generally suitable for exoplanet molecular opacities.

While there has been great progress in the spectroscopy of hot water, the situation is different for methane and ammonia. The key breakthrough for water was the exact variational solution of the vibration–rotation Schrödinger equation using a very high-quality *ab initio* potential energy surface [26] combined with the availability of spectra of the hot molecule [25]. The same approach is underway in several research groups for methane and ammonia; our contribution has been to record high-resolution spectra of hot molecules.

Methane and ammonia are much harder problems than water because there are more atoms so the vibration–rotation problem is much more difficult to solve, and the perturbations between energy levels are much more extensive than those of water (plus the inversion motion in ammonia is an additional complication). For methane, we published a limited set of laboratory data some time ago [8], but the lines have no assignments. The recent calculations for ammonia [29–31] are starting to be useful in assigning hot spectra.

In the interim, we have implemented a 'new' entirely experimental approach for methane and ammonia. The basic idea is straightforward: record infrared and near-infrared emission spectra with a Fourier transform spectrometer at a series of temperatures, calibrate the x- and y-axes to get line positions and intensities in 'real' units (at each measurement temperature) and then fit all the intensities for all temperatures together to determine empirical lower state energies for each line. We thus provide experimental line lists with a line position, line intensity and empirical lower state energy suitable for high-temperature sources, for example exoplanets, and for comparison with theoretical calculations. As these calculations improve, we expect that it will be possible to assign quantum numbers to these data.

We have results for ammonia for 800–2200 cm^{-1} at 0.01 cm^{-1} resolution recorded in emission in two spectral pieces for every 100°C between 300°C and 1300°C plus 1370°C (some 24 high-resolution spectra each with 4000 (low T) to 12 000 lines (high T)) and have published a 'proof-of-principle' paper [32]. These spectra have been recorded with our Bruker IFS 125 HR Fourier transform spectrometer and an evacuated tube furnace source with a flowing ammonia sample (similar to Nassar & Bernath [8]). The relative spectral response has been calibrated with a blackbody source, and the HITRAN database [7] was used to calibrate both the wavenumber and intensity scales.

We have written a computer program that determines empirical lower state energies from the calibrated line intensities using the set of spectra. From the equation above, the ratio S'/S'_0 of line intensities at temperatures T and T_0 is given by

$$\frac{S'}{S'_0} = \frac{Q_0}{Q} \exp\left(\frac{E_{\mathrm{Low}}}{kT_0} - \frac{E_{\mathrm{Low}}}{kT}\right)\left[\frac{1-\exp(-h\nu_{10}/kT)}{1-\exp(-h\nu_{10}/kT_0)}\right].$$

Rearranging and taking the natural logarithm gives the equation

$$\ln\left(\frac{SQ}{S_0Q_0}\left[\frac{1-\exp(-h\nu_{10}/kT_0)}{1-\exp(-h\nu_{10}/kT)}\right]\right) = \ln\left(\frac{SQR_0}{S_0Q_0R}\right) = \frac{E_{\mathrm{Low}}}{kT_0} - \frac{E_{\mathrm{Low}}}{kT},$$

so a plot of $\ln(SQR_0/S_0Q_0R)$ against $1/kT$ yields a straight line. The slope of the fitted line provides the empirical lower state energy (E_{Low}).

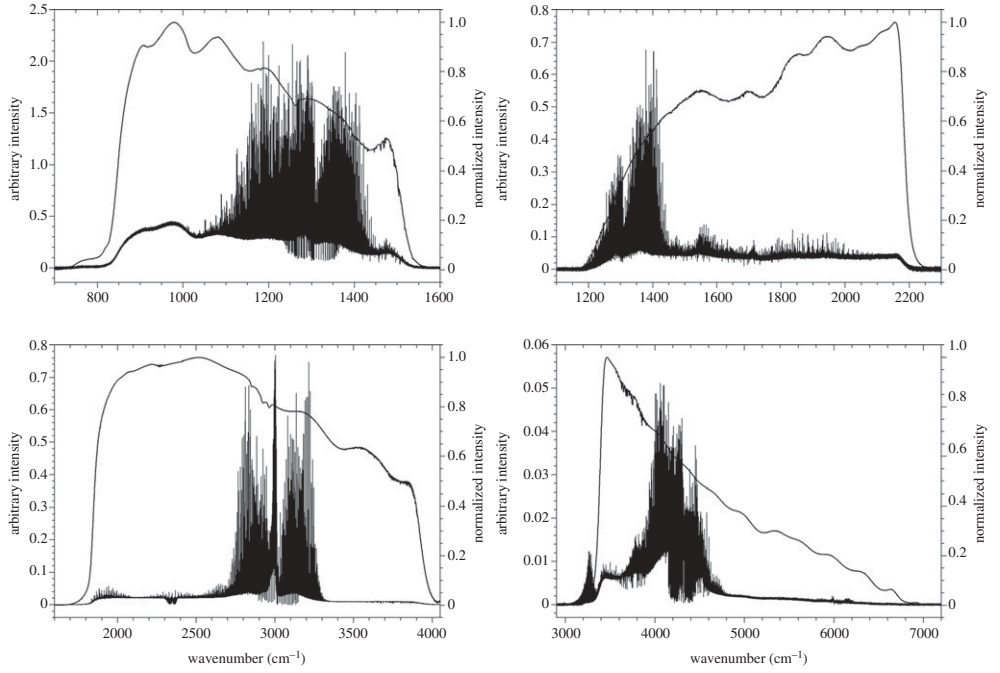

Figure 4. High-resolution laboratory emission spectra of CH_4 at 1000°C for four regions with the corresponding normalized instrument response function. The baseline is caused by residual thermal emission from the tube walls and a small amount of absorption owing to cold CH_4, CO_2 (ν_3 near 2350 cm^{-1}) and H_2O can be seen [38].

A similar method to determine empirical lower state energies has been used by Fortman *et al.* [33] who recorded numerous millimetre wave spectra with the fast scan submillimetre spectroscopic technique as a function of temperature. For NH_3, empirical lower state energies were also determined by Brown & Margolis [34] for unassigned lines in the 4791–5294 cm^{-1} region. Another method has been used recently to obtain lower state energies for near-infrared lines of CH_4 by cooling an absorption cell [35].

By carefully merging our hot line lists with the HITRAN line list, we have created a dataset that can be used over 500–1700 K for 5–13 μm [32]. The final product is a set of 12 line lists (covering 300–1370°C), and each entry in a particular list is a line position, line intensity and lower state energy. To calculate opacities at a particular temperature, the list with the closest temperature is selected and the empirical lower state energies are used to shift the line intensities to match the desired temperature. At 1200°C, our line list has an integrated intensity that is more than a factor of two larger than the HITRAN line list converted to 1200°C (i.e. using HITRAN, which is intended for applications at or below room temperature, results in an error of more than a factor of two in the opacity in this region).

Our data are already being used to improve calculations of the ammonia spectra based on variational solution of the vibration–rotation Schrödinger equation. We sent our line lists in the 800–2200 cm^{-1} region to Tennyson and co-workers at University College London [36] and they have assigned quantum numbers to about 5600 lines (so far about 30% of the observed lines) using the calculations of Yurchenko *et al.* [29]. Ultimately this work will lead to an improved set of theoretical molecular opacities, after the additional empirical adjustment of the potential surface used in the calculation in order to match the observed lines.

In the second paper on NH_3, the adjacent 2100–4000 cm^{-1} region was covered using the same method [37]. The technique was also applied to CH_4 for the temperatures 300–1400°C at twelve 100°C intervals spanning the 960–5000 cm^{-1} region of the infrared [38]. This range encompasses the dyad, pentad and octad regions, i.e. all fundamental vibrational modes along with a number

of combination, overtone and hot bands. As shown in figure 4, the emission spectra were recorded in four overlapping pieces to improve the signal-to-noise ratio. Similar to NH_3, we determined empirical lower state energies of the lines and have a set of 12 line lists covering the 600–1700 K range for 2.0–10.4 μm obtained by combining our emission lines with HITRAN lines.

For CH_4, the theoretical calculations are more difficult than for NH_3 and H_2O, but many research groups are working on the problem [39,40]. As for ammonia, we expect that the theoretical groups will be able to make quantum number assignments in our spectra and will tune the potential energy surfaces to obtain better agreement with laboratory data, with the ultimate goal of obtaining a fully quantum mechanical line list comparable in quality to the BT2 list for water [6].

Our experimental line lists for NH_3 and CH_4 can be used directly for exoplanet spectroscopy. Although they are not as complete as existing theoretical line lists, the line positions from experiment are more accurate. The comparison between experimental and calculated line intensities, however, is more interesting. Experimental line intensities are difficult to obtain because of systematic errors in the measurements, and emission spectra are even more difficult to calibrate than absorption spectra. While state-of-the-art theoretical methods are still many orders of magnitude away from obtaining agreement with experiment line positions for CH_4, NH_3 and H_2O (hence the empirical adjustment of potential energy surfaces), the situation is very different for line intensities. For H_2O, for example, the experimental line intensities (e.g. in HITRAN) typically have errors of a few percent, while it is becoming clear that the line intensities calculated *ab initio* are now substantially better than this [28,41].

4. Conclusion

Molecular opacities are crucial in exoplanet spectroscopy because unreliable spectroscopic data will lead to the retrieval of incorrect compositions and physical properties. The species for which high-temperature data (up to about 2800 K) for hot Jupiters are required include H_2, CO, H_2O, N_2, CH_4, NH_3, CO_2 and HCN; for hot super-Earths additional molecules include SO_2, O_2, HCl, HF, NaCl, KCl, KF, KOH and NaOH. For some species such as CO, CO_2 and H_2O, the existing spectroscopic data are reasonable, although improvements (e.g. high-temperature collisional line broadening parameters) are certainly desirable. Other molecules such as CH_4 and NH_3 are much less satisfactory at high temperatures (and also in the near-infrared spectral region), and considerable experimental and theoretical work is underway to obtain line parameters. Our group has recorded emission spectra of hot CH_4 and NH_3 over a range of temperatures and provided experimental line lists that can be used directly for molecular opacities. Ultimately, the millions of lines needed will have to come from calculations, but laboratory observations have an important role to play.

Funding statement. The author is grateful for the financial support provided by a Research Project Grant from the Leverhulme Trust and from NASA.

References

1. Mayor M, Queloz D. 1995 A Jupiter-mass companion to a solar type star. *Nature* **378**, 355–359. (doi:10.1038/378355a0)
2. Mason JW (ed.) 2008 *Exoplanets: detection, formation, properties, habitability*. Chichester, UK: Praxis Publishing.
3. Charbonneau D, Brown TM, Latham DW, Mayor M. 2000 Detection of planetary transits across a Sun-like star. *Astrophys. J. Lett.* **529**, L45–L48. (doi:10.1086/312457)
4. Batalha NM *et al*. 2013 Planetary candidates observed by Kepler. III. Analysis of the first 16 months of data. *Astrophys. J. Suppl. Ser.* **204**, 24. (doi:10.1088/0067-0049/204/2/24)
5. Swain MR, Vasisht G, Tinetti G. 2008 The presence of methane in the atmosphere of an extrasolar planet. *Nature* **452**, 329–331. (doi:10.1038/nature06823)
6. Barber RJ, Tennyson J, Harris GJ, Tolchenov RN. 2006 A high-accuracy computed water line list. *Mon. Not. R. Astron. Soc.* **368**, 1087–1094. (doi:10.1111/j.1365-2966.2006.10184.x)

7. Rothman LS *et al*. 2009 The HITRAN 2008 molecular spectroscopic database. *J. Quant. Spectrosc. Radiat. Transf.* **110**, 533–572. (doi:10.1016/j.jqsrt.2009.02.013)
8. Nassar R, Bernath P. 2003 Hot methane spectra for astrophysical applications. *J. Quant. Spectrosc. Radiat. Transf.* **82**, 279–292. (doi:10.1016/S0022-4073(03)00158-4)
9. Swain MR, Vasisht G, Tinetti G, Bouwman J, Chen P, Yung Y, Deming D, Deroo P. 2009 Molecular signatures in the near-infrared dayside spectrum of HD 189733b. *Astrophys. J. Lett.* **690**, L114–L117. (doi:10.1088/0004-637X/690/2/L114)
10. Grillmair CJ, Burrows A, Charbonneau D, Armus L, Stauffer J, Meadows V, van Cleve J, von Braun K, Levine D. 2008 Strong water absorption in the dayside emission spectrum of the planet HD 189733b. *Nature* **456**, 767–769. (doi:10.1038/nature07574)
11. Waldmann IP, Drossart P, Tinetti G, Griffith CA, Swain M, Deroo P. 2012 Ground-based near-infrared emission spectroscopy of HD 189733b. *Astrophys. J.* **744**, 35. (doi:10.1088/0004-637X/744/1/35)
12. Seager S, Deming D. 2010 Exoplanet atmospheres. *Annu. Rev. Astron. Astrophys.* **48**, 631–672. (doi:10.1146/annurev-astro-081309-130837)
13. Hand E. 2011 Super-Earths give theorists a super headache. *Nature* **480**, 302. (doi:10.1038/480302a)
14. Schaefer L, Lodders K, Fegley B. 2012 Vaporization of the Earth: application to exoplanet atmospheres. *Astrophys. J.* **755**, 41. (doi:10.1088/0004-637X/755/1/41)
15. Lee J-M, Fletcher LN, Irwin PGJ. 2012 Optimal estimation retrievals of the atmospheric structure and composition of HD 189733b from secondary eclipse spectroscopy. *Mon. Not. R. Astron. Soc.* **420**, 170–182. (doi:10.1111/j.1365-2966.2011.20013.x)
16. Showman AP, Fortney JJ, Lian Y, Marley MS, Freedman RS, Knutson HA, Charbonneau D. 2009 Atmospheric circulation of hot Jupiters: coupled radiative-dynamical general circulation model simulations of HD 189733b and HD 209458b. *Astrophys. J.* **699**, 564–584. (doi:10.1088/0004-637X/699/1/564)
17. Venot O, Hébrard E, Agúndez M, Dobrijevic M, Selsis F, Hersant F, Iro N, Bounaceur R. 2012 A chemical model for the atmosphere of hot Jupiters. *Astron. Astrophys.* **546**, A43. (doi:10.1051/0004-6361/201219310)
18. Hatzes AP *et al*. 2011 The mass of CoRoT-7b. *Astrophys. J.* **743**, 75. (doi:10.1088/0004-637X/743/1/75)
19. Bernath PF. 2005 *Spectra of atoms and molecules*. New York, NY: Oxford University Press.
20. Fischer J, Gamache RR. 2002 Total internal partition sums for molecules of astrophysical interest. *J. Quant. Spectrosc. Radiat. Transf.* **74**, 263–272. (doi:10.1016/S0022-4073(01)00234-5)
21. Sharp CM, Burrows A. 2007 Atomic and molecular opacities for brown dwarf and giant planet atmospheres. *Astrophys. J. Suppl. Ser.* **168**, 140–166. (doi:10.1086/508708)
22. Tennyson J, Yurchenko SN. 2012 ExoMol: molecular line lists for exoplanet and other atmospheres. *Mon. Not. R. Astron. Soc.* **425**, 21–33. (doi:10.1111/j.1365-2966.2012.21440.x)
23. Rothman LS, Gordon IE, Barber RJ, Dothe H, Gamache RR, Goldman A, Perevalov VI, Tashkun SA, Tennyson J. 2010 HITEMP, the high-temperature molecular spectroscopic database. *J. Quant. Spectrosc. Radiat. Transf.* **111**, 2139–2150. (doi:10.1016/j.jqsrt.2010.05.001)
24. Hase F, Wallace L, McLeod SD, Harrison JJ, Bernath PF. 2010 The ACE-FTS atlas of the infrared solar spectrum. *J. Quant. Spectrosc. Radiat. Transf.* **111**, 521–528. (doi:10.1016/j.jqsrt.2009.10.020)
25. Wallace L, Bernath P, Livingston W, Hinkle K, Busler J, Guo B, Zhang K-Q. 1995 Water on the Sun. *Science* **268**, 1155–1158. (doi:10.1126/science.7761830)
26. Polyansky OL, Zobov NF, Viti S, Tennyson J, Bernath PF, Wallace L. 1997 Water on the Sun: line assignments based on variational calculations. *Science* **277**, 346–348. (doi:10.1126/science.277.5324.346)
27. Tennyson J *et al*. 2013 IUPAC critical evaluation of the rotational–vibrational spectra of water vapor. III. Energy levels and transition wavenumbers for $H_2^{16}O$. *J. Quant. Spectrosc. Radiat. Transf.* **117**, 29–58. (doi:10.1016/j.jqsrt.2012.10.002)
28. Polyansky OL, Zobov NF, Mizus II, Lodi L, Yurchenko SN, Tennyson J, Császár AG, Boyarkin OV. 2012 Global spectroscopy of the water monomer. *Phil. Trans. R. Soc. A* **370**, 2728–2748. (doi:10.1098/rsta.2011.0259)
29. Yurchenko SN, Barber RJ, Tennyson J. 2011 A variationally computed line list for hot NH_3. *Mon. Not. R. Astron. Soc.* **413**, 1828–1834. (doi:10.1111/j.1365-2966.2011.18261.x)
30. Huang X, Schwenke DW, Lee T. 2011 Rovibrational spectra of ammonia. I. Unprecedented accuracy of a potential energy surface used with nonadiabatic corrections. *J. Chem. Phys.* **134**, 044320. (doi:10.1063/1.3541351)

31. Huang X, Schwenke DW, Lee T. 2011 Rovibrational spectra of ammonia. II. Detailed analysis, comparison, and prediction of spectroscopic assignments for $^{14}NH_3$, $^{15}NH_3$, and $^{14}ND_3$. *J. Chem. Phys.* **134**, 044321. (doi:10.1063/1.3541352)
32. Hargreaves R, Li G, Bernath PF. 2011 Hot NH_3 spectra for astrophysical applications. *Astrophys. J.* **735**, 111. (doi:10.1088/0004-637X/735/2/111)
33. Fortman SM, Medvedev IR, Neese CF, De Lucia FC. 2010 A new approach to astrophysical spectra: the complete experimental spectrum of ethyl cyanide (CH_3CH_2CN) between 570 and 645 GHz. *Astrophys. J.* **714**, 476–486. (doi:10.1088/0004-637X/714/1/476)
34. Brown LR, Margolis JS. 1996 Empirical line parameters of NH_3 from 4791 to 5294 cm^{-1}. *J. Quant. Spectrosc. Radiat. Transf.* **56**, 283–294. (doi:10.1016/0022-4073(96)00041-6)
35. Wang L, Kassi S, Liu AW, Hu SM, Campargue A. 2010 High sensitivity absorption spectroscopy of methane at 80 K in the 1.58 μm transparency window: temperature dependence and importance of the CH_3D contribution. *J. Mol. Spectrosc.* **261**, 41–52. (doi:10.1016/j.jms.2010.02.005)
36. Zobov NF, Shirin SV, Ovsyannikov RI, Polyansky OL, Yurchenko SN, Barber RJ, Tennyson J, Hargreaves R, Bernath PF. 2011 Analysis of high temperature ammonia spectra from 780 to 2100 cm^{-1}. *J. Mol. Spectrosc.* **269**, 104–108. (doi:10.1016/j.jms.2011.05.003)
37. Hargreaves R, Li G, Bernath PF. 2012 Ammonia line lists from 1650 to 4000 cm^{-1}. *J. Quant. Spectrosc. Radiat. Transf.* **113**, 670–679. (doi:10.1016/j.jqsrt.2012.02.033)
38. Hargreaves RJ, Beale CA, Michaux L, Irfan M, Bernath PF. 2012 Hot methane line lists for exoplanet and brown dwarf atmospheres. *Astrophys. J.* **757**, 46. (doi:10.1088/0004-637X/757/1/46)
39. Warmbier R, Schneider R, Sharma AR, Braams BJ, Bowman JM, Hauschildt PH. 2009 Ab initio modeling of molecular IR spectra of astrophysical interest: application to CH_4. *Astron. Astrophys.* **495**, 655–661. (doi:10.1051/0004-6361:200810983)
40. Nikitin AV, Rey M, Tyuterev VG. 2011 Rotational and vibrational energy levels of methane calculated from a new potential energy surface. *Chem. Phys. Lett.* **501**, 179–186. (doi:10.1016/j.cplett.2010.11.008)
41. Lodi L, Tennyson J, Polyansky OL. 2011 A global, high accuracy *ab initio* dipole moment surface for the electronic ground state of the water molecule. *J. Chem. Phys.* **135**, 034113. (doi:10.1063/1.3604934)